



NATURAL FREQUENCY ERROR ESTIMATION USING A PATCH RECOVERY TECHNIQUE

D. B. STEPHEN AND G. P. STEVEN

*Finite Element Analysis Research Centre, Building J07, Engineering Faculty,
University of Sydney, N.S.W. 2006, Australia*

(Received 10 July 1995, and in final form 26 June 1996)

In computing eigenvalues for a large finite element system, it has been observed that the eigenvalue extractors produce eigenvectors that are in some sense more accurate than their corresponding eigenvalues. In this paper, computational examples are presented to validate this observation. From this observation, a patch type technique is developed based on the eigenvector for one mesh quality to provide an eigenvalue error indicator. Tests show this indicator to be both accurate and reliable.

This technique was first observed by Stephen and Steven for an error estimation for buckling and has been extended in this paper to predict an error for the natural frequency finite element analysis of a structure.

© 1997 Academic Press Limited

1. INTRODUCTION

The finite element method discretizes a structure into relatively simple elements to represent a more complex model. The prime source of error in the finite element analysis is from this discretization, in which the displacements of the simple elements attempt to represent a complex distorted shape.

It demonstrated using computational examples, by Stephen and Steven [1], that the eigenvector solution to a finite element analysis is more accurate than the eigenvalue. It is the eigenvalue solution that is required in a finite element analysis, so any error indicator should use the more accurate eigenvector solution to determine an error estimate for the analysis. There is no current mathematical proof that the eigenvector is more accurate than the eigenvalue. Strang and Fix [2] base their error estimation on the eigenfunctions rather than the eigenvectors. However, Dupont and Douglas [3] prove that the nodal quantities in a linear static analysis are the accurate points and, as the linear static matrices are used in vibration analysis, it can be expected that the nodal points will be the accurate displacement locations for the vibration analysis.

Stephen and Steven [1] derived an error measure for the buckling finite element analysis based on the more accurate eigenvector solution. In this paper the same principle is extended to natural frequency finite element analysis, to estimate the error on the natural frequency given by the square root of the eigenvalue.

The eigenvalue can be calculated from global elastic stiffness and mass matrices using the Rayleigh quotient as follows:

$$\lambda = \frac{\{x\}^T [K] \{x\}}{\{x\}^T [M] \{x\}}. \quad (1)$$

Given that the eigenvector is a more accurate quantity than the eigenvalue, the elastic stiffness and mass matrices will determine the level or accuracy of the solution. These matrices are a result of the shape function and element type used in their compilation.

2. PATCH RECOVERY

The patch recovery technique for improved stress retrieval of a statical analysis has been researched for several years [4–7]. This procedure involves taking a patch of elements around the point of concern in the finite element model and interpolating more accurate solutions from the optimum accuracy stress locations on the elements in the patch. These locations were generally found to be the Gauss points of the elements [8].

The finite element natural frequency analysis has the eigenvector being the more accurate nodal quantity; hence a more accurate solution is achieved by interpolation over the patch using the nodal displacement quantities. This procedure has been previously examined for buckling finite element analysis [2, 3].

A finite element has sufficient nodal quantities to produce a vibrating shape equal to its polynomial shape function. A high order polynomial function over the element which is of higher order than the shape function will produce a more accurate vibrating shape. This high order polynomial function can be easily produced by a least squares procedure incorporating the eigenvector solution of the nodes of the element and the surrounding elements in the patch.

For a one-dimensional model consisting of beam elements, a patch can have either two elements or three elements, as shown in Figure 1. Each node in a beam element has two degrees of freedom, being the displacement and the rotation of the node. A standard beam element contains two nodes totalling four degrees of freedom. The order of the polynomial shape function for this element is three.

For the case of the two-element patch, there is a total of six degrees of freedom. A polynomial of order five can be interpolated over the central patch element. The three-element patch has eight degrees of freedom for a polynomial of order seven over the central patch element.

In two-dimensional structures consisting of membrane elements there can be many elements and nodes in a patch: see Figure 2. Attempting to fit very high order polynomials to the patch often leads to singularities in the matrix for the interpolation function, or the interpolation function produces additional waves inside the element. A higher order polynomial than the element shape function and a lower order polynomial than using every node in the patch can be achieved efficiently using the method of least squares.

Fitting a weighted least squares polynomial to the vibrating shape over the patch of elements was found to produce better results than an ordinary least squares polynomial approximation. The weighting produces a function that is more dependent on the

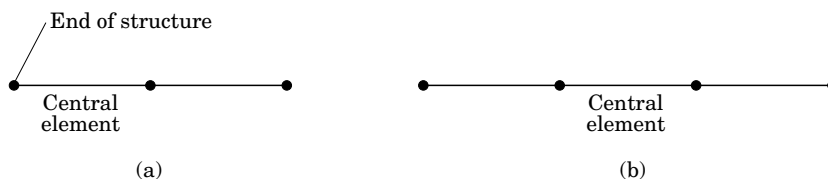


Figure 1. The beam element patches. (a) Two-element patch; (b) three-element patch.

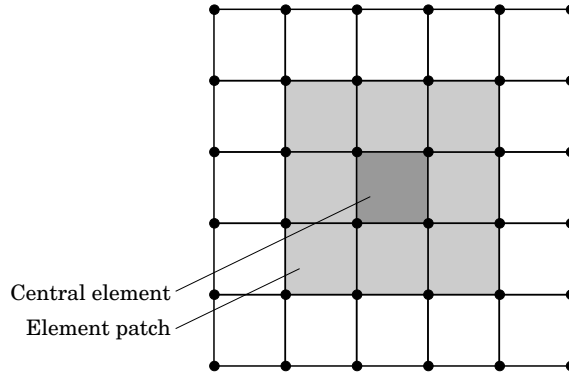


Figure 2. The 2-D element patch.

elemental nodes compared to the surrounding nodes in the patch. For elements on rigid boundaries, where the exact value is known to be zero displacement, this weighting has a more desirable effect. The optimal weighting for the least squares was found when each term was multiplied by the square root of the distance to each node from the centroid of the element in question.

It is assumed that the higher order polynomial function on each element gives a more accurate result for the vibrating shape. To calculate a more accurate eigenvalue solution, each element is divided into sub-elements, with nodal displacements obtained from the higher order function shown in Figure 3.

A new eigenvalue λ^* can be calculated using the Rayleigh quotient at the sub-elemental level. The Rayleigh quotient can be written as the summation of the sub-elemental contributions, as

$$\lambda^* = \left[\sum_{i=1}^N \sum_{j=1}^N u_i(k)_{i,j} u_j \right] / \left[\sum_{i=1}^N \sum_{j=1}^N u_i(m)_{i,j} u_j \right]. \quad (2)$$

In equation (2) there is a total of N degrees of freedom; u_i represents the displacement quantities for the patch nodes, with $(k)_{i,j}$ and $(m)_{i,j}$ representing the terms in the elastic stiffness and mass matrices respectively. This result allows each element to have its patch in the modal identified, the higher order function determined and the Rayleigh quotient summations calculated. Upon the completion of this process for each element in the model, the new eigenvalue can be calculated.

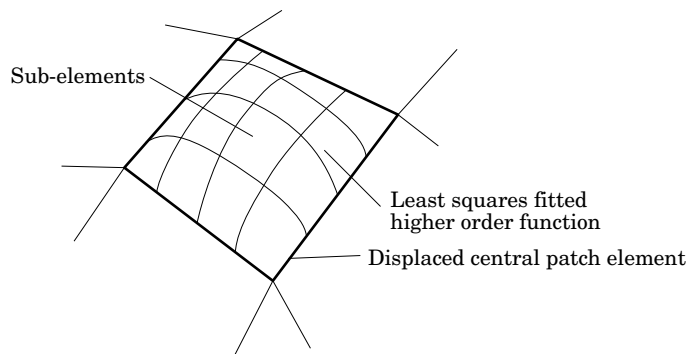


Figure 3. Sub-elements on the original patch element.

3. HIGHER ORDER FUNCTIONS

The finite element shape functions are generally of a low polynomial order with respect to the complex deformed shapes of vibrating structures. The simple one-dimensional vibrating string has the deformed shape of a sine curve which, when using a Taylor series expansion, is an infinite order polynomial expansion. The simple one-dimensional elements, usually only having a linear shape function, can never perfectly represent this deformed shape. These simple shape functions can only form linear intervals over the deformed shape. Use of a quadratic function can better represent the curved shape of the true deformed shape.

To examine the effect of the least squares interpolation function compared to the finite element shape function, a sine curve was used as the exact deformed shape. The errors were measured as norms with respect to the displaced shape and the first differential of the function. The displacement error norm was calculated as

$$\|e_u\| = \int_0^h (F(x) - f(x))^2 dx$$

where $F(x)$ is the exact displacement function, $f(x)$ is the approximate displacement function, being either the finite element shape function or the least squares interpolation, and h is the length of the element. The differential error norm was similarly calculated as

$$\|e_u'\| = \int_0^h (F'(x) - f'(x))^2 dx$$

The least squares displacement function was calculated over a patch of three elements. This included the displacements for a total of four nodes. The weighting for the terms in the least squares was taken as the inverse of the distance from the central element centroid to the particular node squared. The patch over the three elements is represented in Figure 4.

A cubic function could be calculated using these nodes; however, only a quadratic was used as the Taylor series expansion of the sine curve results in non-even powers of the polynomial terms, and a quadratic should be less accurate than a cubic function for the sine curve. Hence this method shows significant improvement for the higher order polynomials that are not part of the true displacement function.

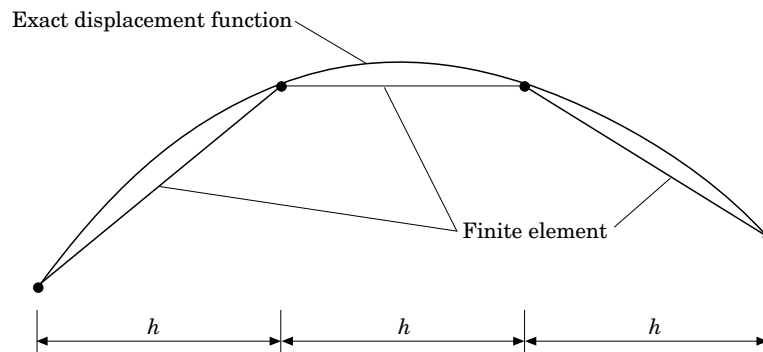


Figure 4. The three element patch.

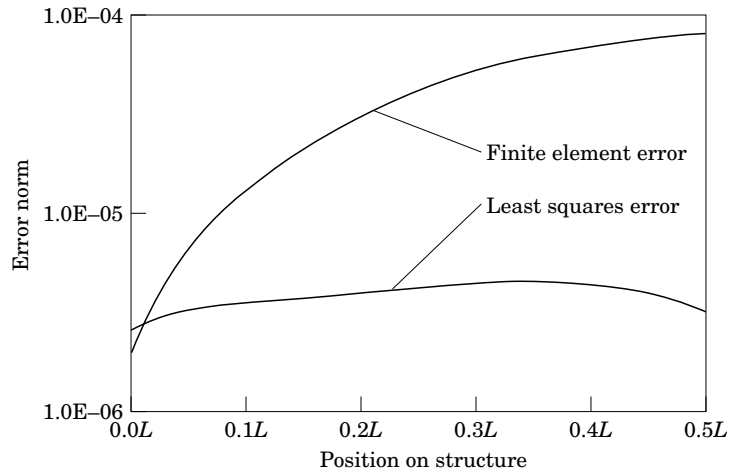


Figure 5. The displacement error norm.

The system was analysed from 0 to $\pi/2$ over the sine displacement curve. The element could be placed at any position on this interval. The element size was chosen to be 0.1π . Differential sizes have the same relationship: only the magnitudes of the norms differed.

The displacement error norm is plotted in Figure 5.

The differential error norm is plotted in Figure 6. This value corresponds with the stresses in the structure and translates to the numerator of the Rayleigh quotient, whereas the displacements correspond with the denominator.

In both cases the error norm from the least squares function is less than the finite element shape function, except at positions close to the start of the structure, where the values are almost the same.

Hence using a higher order polynomial than the finite element shape functions defines a more accurate displaced shape for both the displacement and first differential.

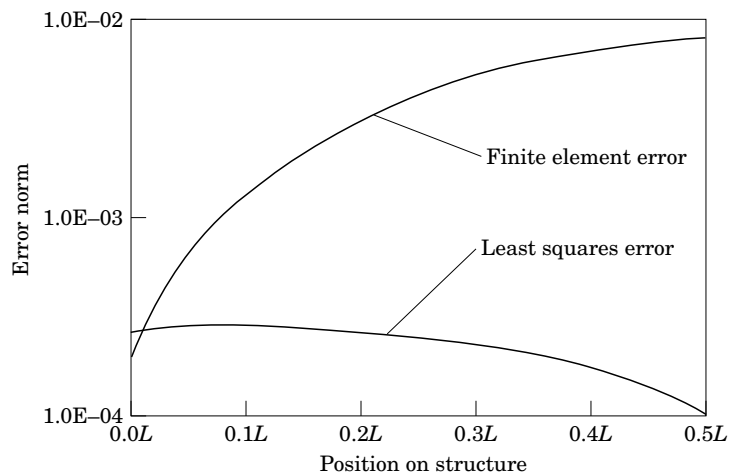


Figure 6. The differential error norm.

4. ERROR MEASURE

The new eigenvalue obtained from the higher order polynomial equations on each element is more accurate than the original finite element solution due to the higher order function used to quantify the vibrating shape and smoothing process involved, with application of a least squares fit of the displaced shapes to a larger region than the single element of concern.

This improved solution is not exact, due to the true vibrating shape being even more complex than the higher order polynomial, and that there is no guarantee that the higher order polynomial is defined from exact quantities. The improved eigenvalue may best be used as an error measure for the analysis.

The error for the finite element analysis is written as

$$\varepsilon_\lambda = (\lambda^{FE} - \lambda)/\lambda. \quad (3)$$

In most cases, the exact eigenvalue λ is unknown, so it may be replaced with the improved eigenvalue λ^* to give an error estimate based on this value to represent the actual error. This error estimate is expressed as

$$\varepsilon^* = (\lambda^{FE} - \lambda^*)/\lambda^*. \quad (4)$$

5. EXAMPLES

5.1. SIMPLY SUPPORTED BEAM

A simply supported beam was created using equal length beam elements: see Figure 7. The structure was analysed for its natural frequencies with a variety of mesh sizes.

The exact eigenvalue for this problem for mode r is

$$\lambda = (r\pi)^4 \frac{EI}{mL^4}. \quad (5)$$

The natural frequency is the square root of the eigenvalue. The eigenvalue error is plotted in Figure 8 for the first two modes with various mesh sizes. The figure also contains the improved eigenvalue error and the measure of the finite element error using the improved eigenvalue. For the patch recovery of the improved eigenvalue, each element in the models examined was divided into five sub-elements.

Note that the improved eigenvalues have a higher convergence rate than the convergence rate of the finite element eigenvalue alone. This indicates the high accuracy of the eigenvector solution.

The error measure for both modes gives a highly accurate approximation to the true error. The differences between the error of the eigenvector for finite element solution and the error measure based upon the improved eigenvalue are virtually negligible.

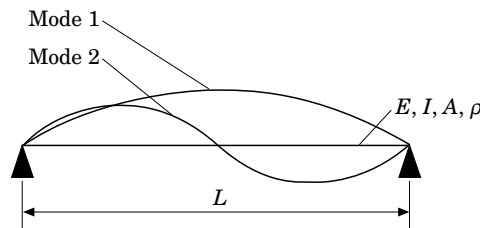


Figure 7. The simply supported beam.

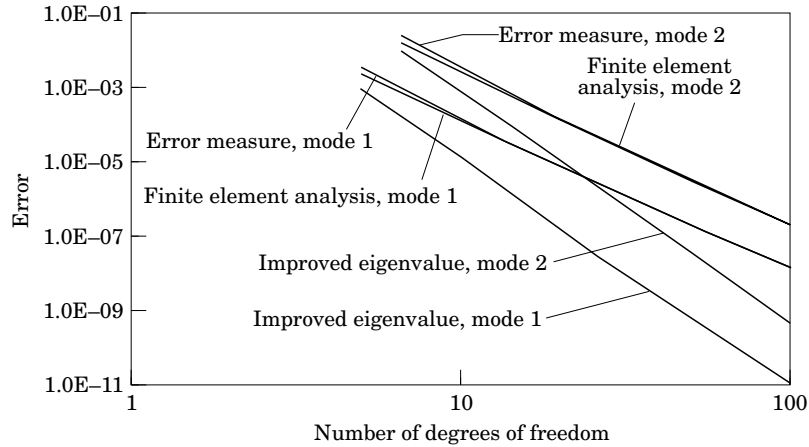


Figure 8. Finite element and improved eigenvalue errors for the simply supported beam natural frequency.

5.2. CANTILEVERING BEAM

A rigidly fixed base cantilevering beam was created using isoparametric, constant stress membrane elements. The structure was analyzed for the first four natural frequencies in bending, with a variety of mesh sizes. The Young's modulus and density of this material used to model the structure was set to unity. The Poisson ratio was 0.25. This structure is shown in Figure 9 and the first four bending vibration modes are shown in Figures 10(a)–(d).

Natural frequency analysis using the finite element method can be performed using either a consistent or a lumped mass matrix. The choice of the mass matrix can affect the convergence of the analysis. As there are two types of mass matrices, the improved eigenvalue was calculated using both types. The graphs of the errors in the finite element and improved eigenvalues are plotted in Figures 11–18 for the first four mode bending vibration modes, for both the consistent and lumped mass matrices. The finite element error is based upon calculating the exact eigenvalue from a number of mesh refinements and extrapolating the exact eigenvalue. The error measure is based upon the improved eigenvalue from the patch recovery.

This process involves subdividing every element in the model into a specific number of sub-elements. From discretization it is known that the higher the number of elements is, the more accurate the solution will be. Increasing the number of sub-elements also increases the time of computation of the new eigenvalue. The improved vibrating surface will not be exact, as the higher order polynomial used cannot exactly represent an even higher order function for the vibrating shape. Therefore, having infinitesimally

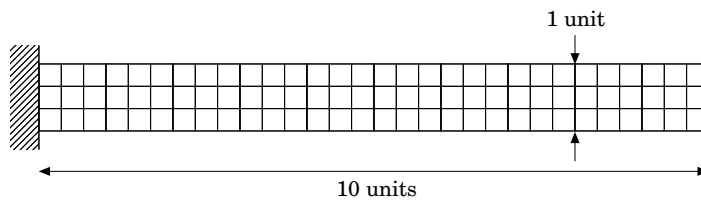


Figure 9. The cantilever beam model with and compressive load.

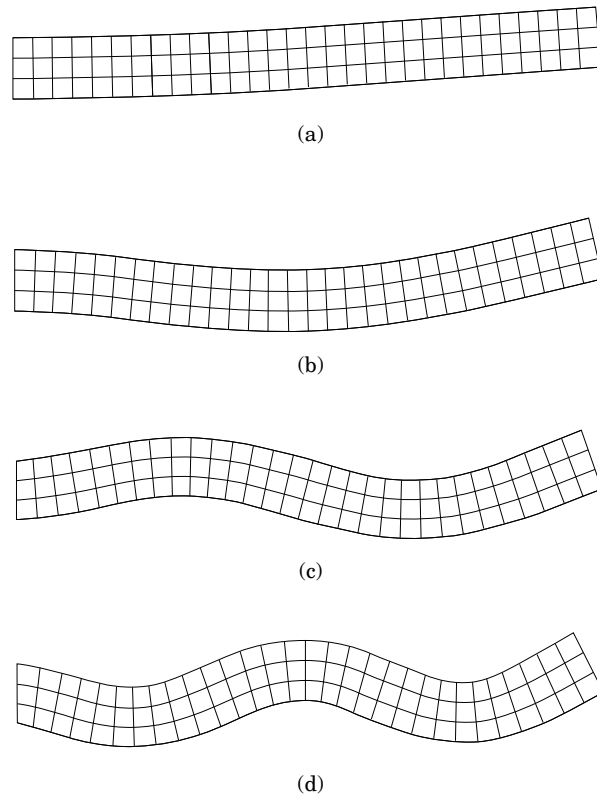


Figure 10. The vibrating cantilever. (a) Mode 1; (b) mode 2; (c) mode 3; (d) mode 4.

small sub-elements to achieve the exact shape of the new vibrating shape is of no real benefit. A sub-mesh of 5×5 for the patch technique was used for each element in this example.

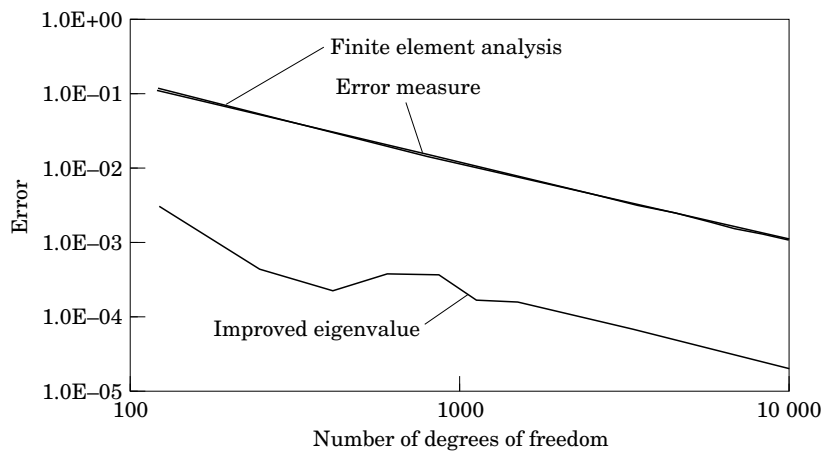


Figure 11. Finite element analysis and improved eigenvalue errors for the cantilevering beam: consistent mass matrix, mode 1.

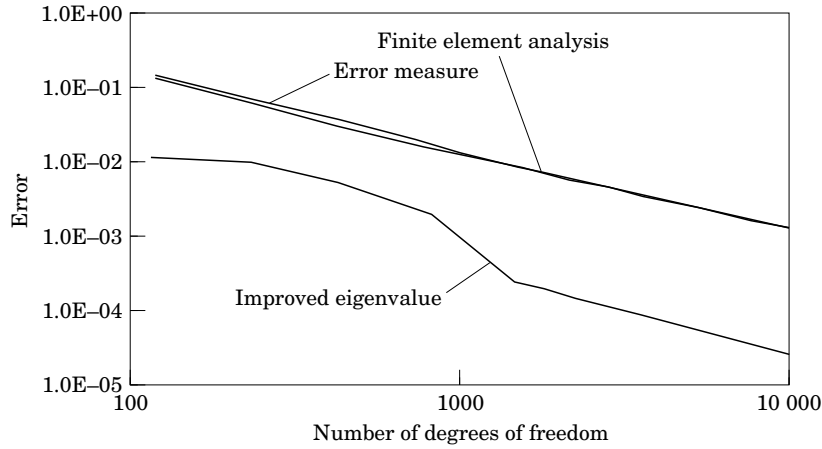


Figure 12. Finite element analysis and improved eigenvalue errors for the cantilevering beam: consistent mass matrix, mode 2.

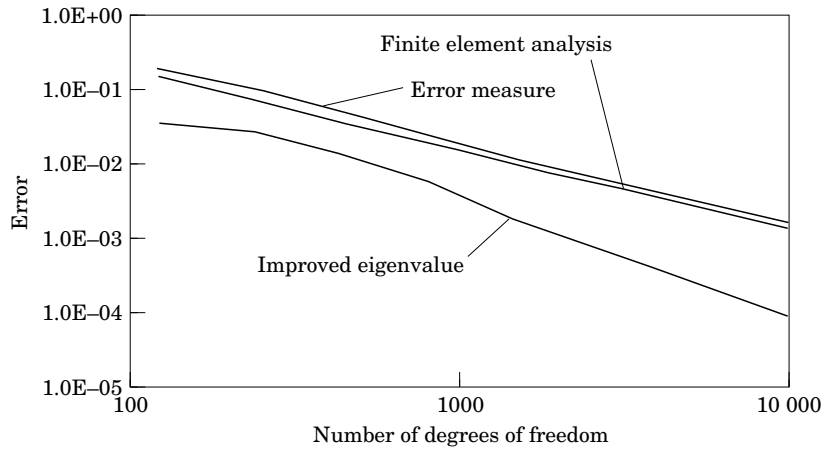


Figure 13. Finite element analysis and improved eigenvalue errors for the cantilevering beam: consistent mass matrix, mode 3.

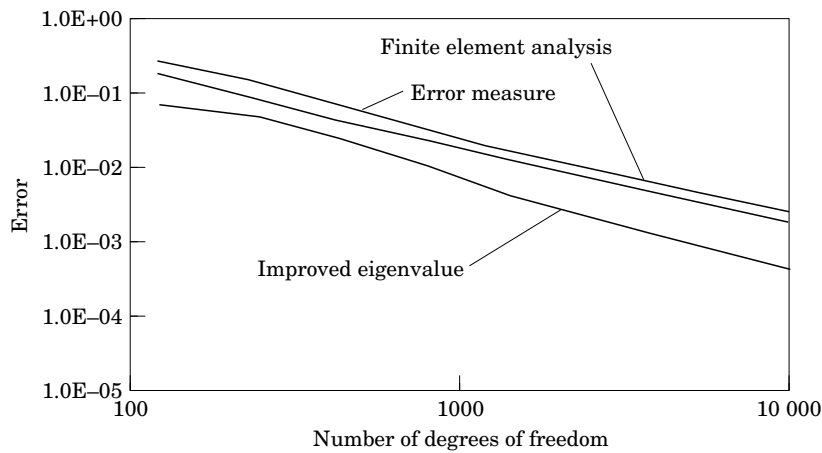


Figure 14. Finite element analysis and improved eigenvalue errors for the cantilevering beam: consistent mass matrix, mode 4.

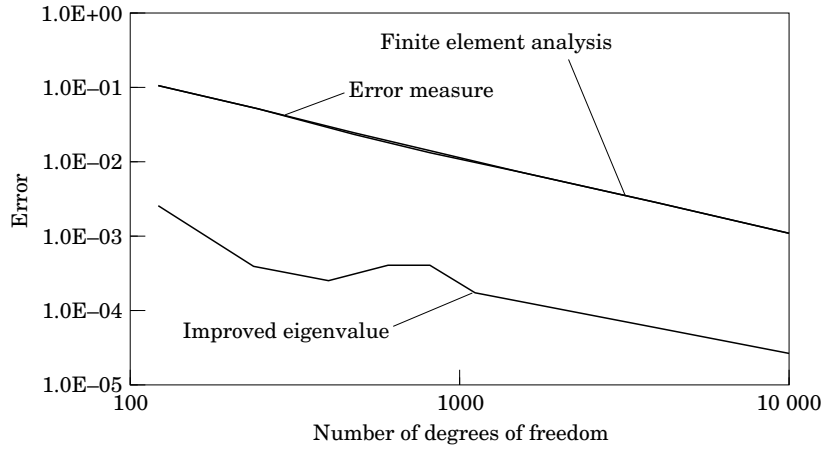


Figure 15. Finite element analysis and improved eigenvalue errors for the cantilevering beam: lumped mass matrix, mode 1.

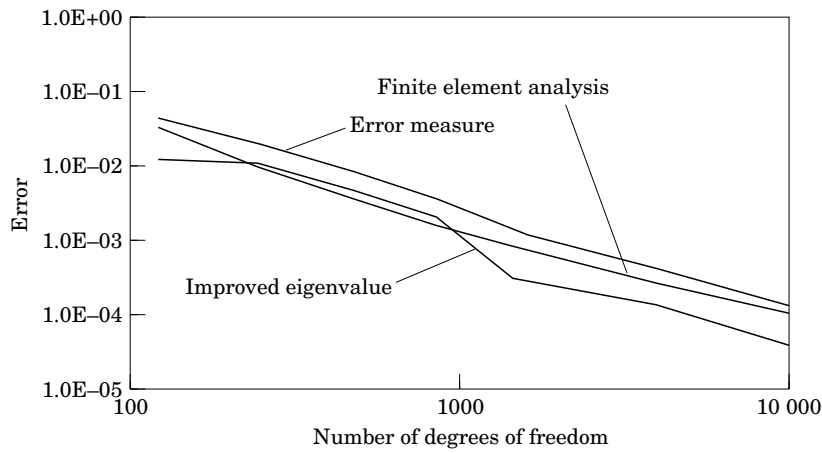


Figure 16. Finite element analysis and improved eigenvalue errors for the cantilevering beam: lumped mass matrix, mode 2.

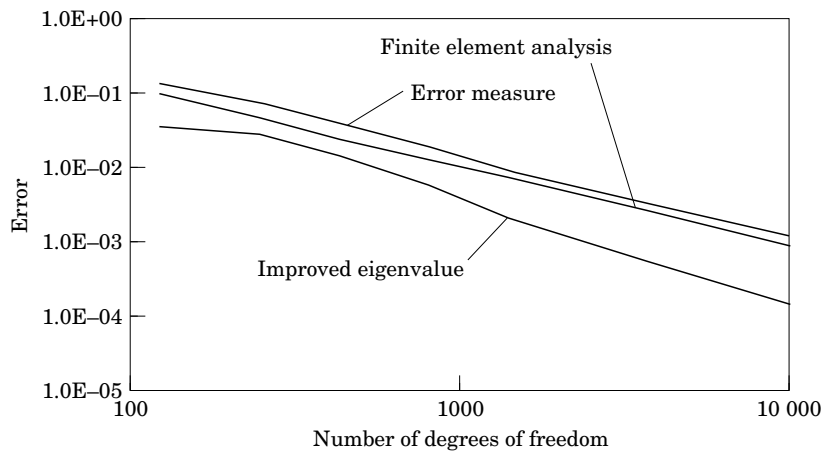


Figure 17. Finite element analysis and improved eigenvalue errors for the cantilevering beam: lumped mass matrix, mode 3.

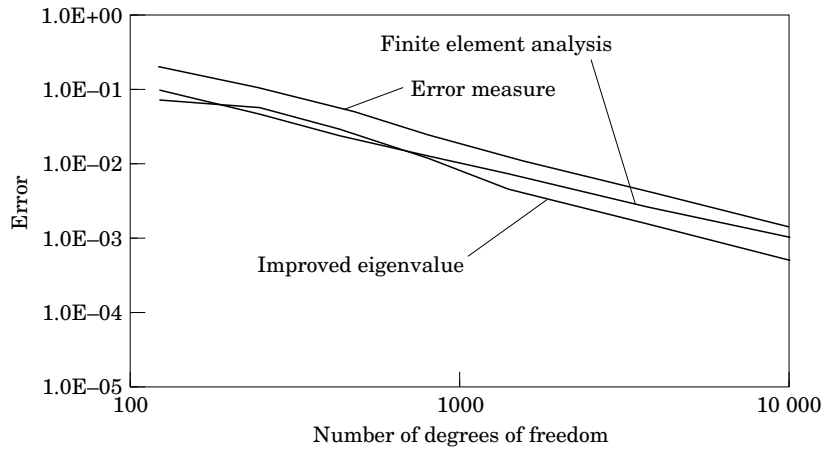


Figure 18. Finite element analysis and improved eigenvalue errors for the cantilevering beam: lumped mass matrix, mode 4.

The improved eigenvalues for modes 1 and 2 for the consistent mass matrices and mode 1 for the lumped matrices models produced an error measure almost identical to the finite element analysis error.

The improved eigenvalues for modes 3 and 4 for the consistent mass matrices and modes 2, 3 and 4 for the lumped mass matrices were not as accurate as the other lower modes. However, the error measure gave a good estimate of the eigenvalue error for the finite element analysis. This is due to the patch technique producing the improved eigenvalues having a convergence rate opposite to that of the finite element analysis. For example, if the finite element analysis converges to the exact solution from above, the patch improved eigenvalue converges from below. As a result of this different convergence rate, the error measure produced is a conservative value.

The patch recovery technique gave accurate estimations for both consistent and lumped mass matrices analyses.

5.3. PORTAL FRAME

A portal frame consisting of membrane elements was analyzed with various element subdivisions. Again isoparametric, constant stress, membrane elements were used to model this structure, with the Young's modulus and density of this material set to unity. The

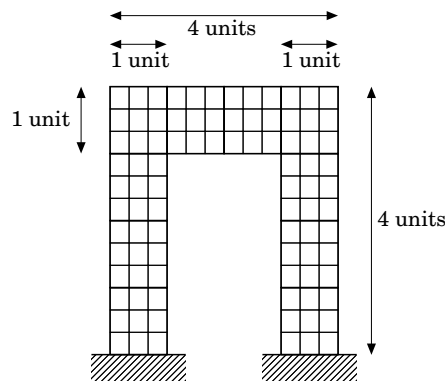


Figure 19. The portal frame model from membrane elements.

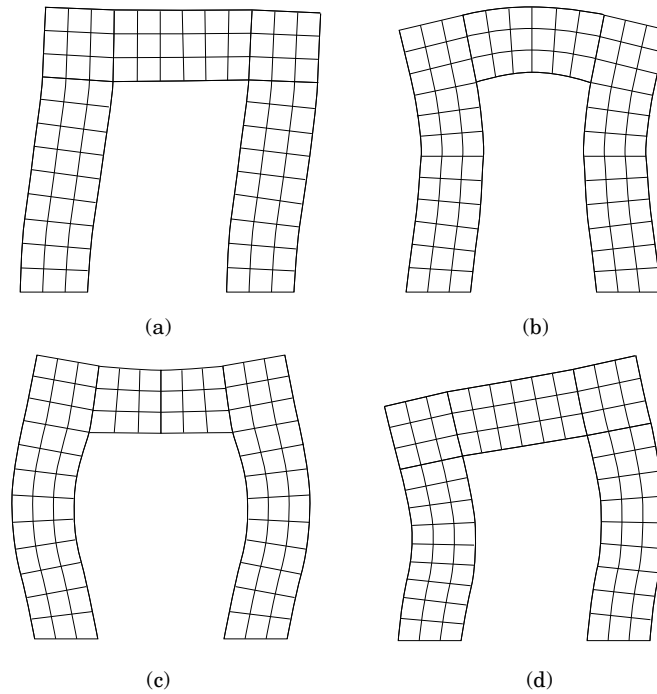


Figure 20. The vibrating portal frame. (a) Mode 1; (b) mode 2; (c) mode 3; (d) mode 4.

Poisson ratio was again 0.25. The structure is represented in Figure 19 and the vibrating shapes are shown in Figures 20(a)–(d).

The eigenvalue for the finite element analysis and the improved value are plotted in Figures 21–24. The error measure for the finite element analysis based on the improved eigenvalue is also plotted in these figures.

Modes 1 and 3 produced improved eigenvalues that were quite accurate and gave extremely good error measures for the finite element analysis. Modes 2 and 4 had improved

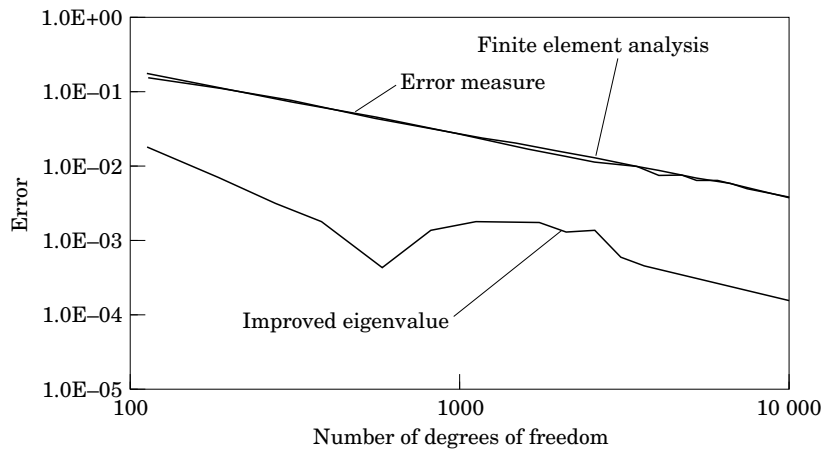


Figure 21. Finite element analysis and improved eigenvalue errors for the portal frame example: lumped mass matrix, mode 1.

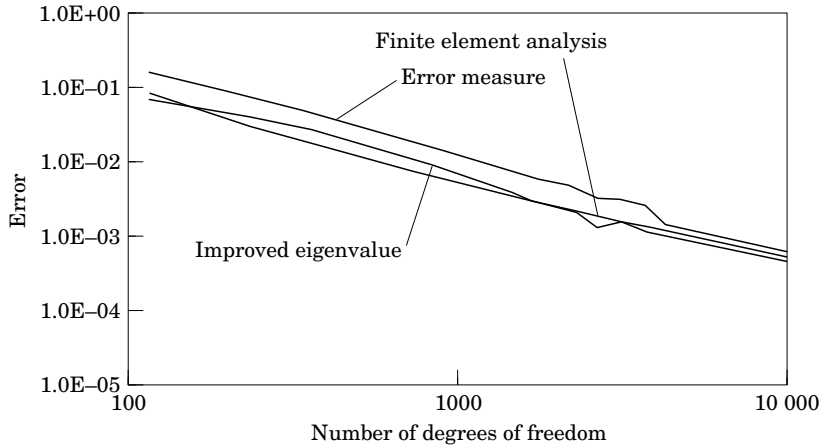


Figure 22. Finite element analysis and improved eigenvalue errors for the portal frame example: lumped mass matrix, mode 2.

eigenvalues that were similar in accuracy to the finite element analysis. However, as in the cantilevering beam example, the improved eigenvalue converged to the exact solution from the opposite way to the finite element eigenvalue. Hence conservative error estimates were again produced.

6. COMMENTS

The finite element analysis eigenvalue error is calculated based upon the exact solution. In most practical cases the exact solution cannot be found without several analyses and extrapolation of the exact solution. This is time consuming and costly for practical use. The error measure is based upon the improved eigenvalue using the patch recovery technique. It needs only to examine the original finite element solution. It is therefore a suitable method of estimating the eigenvalue error in a finite element analysis.

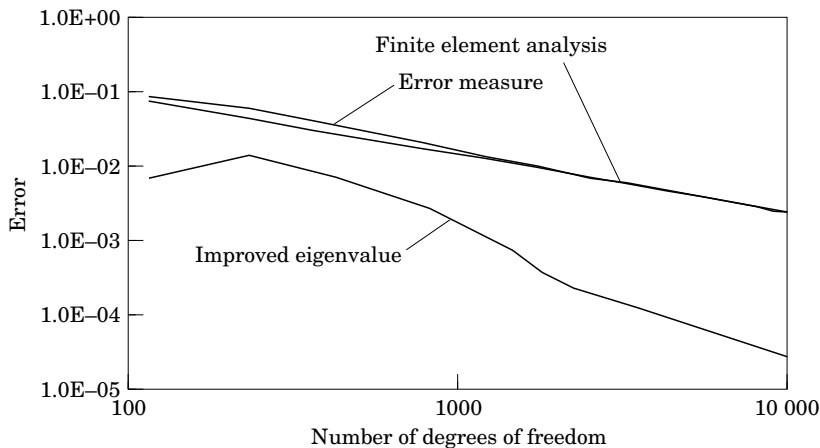


Figure 23. Finite element analysis and improved eigenvalue errors for the portal frame example: lumped mass matrix, mode 3.

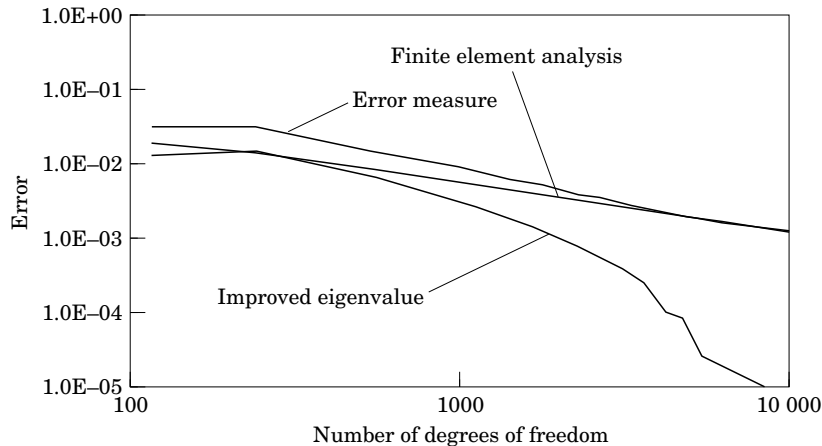


Figure 24. Finite element analysis and improved eigenvalue errors for the portal frame example: lumped mass matrix, mode 4.

The error measure quite accurately estimates the finite element eigenvalue error. This can be seen, as the error for the finite element analysis eigenvalue almost identically coincides with the error measure.

To compute the improved eigenvalue using this technique in a vibration type finite element analysis, one examines a patch of elements around each element individually. A weighted least squares function is calculated for the displacement over the patch of elements using the nodal point displacements given by the original finite element analysis. The central element of the patch is subdivided into a more refined mesh and the nodal displacements are calculated from the least squares function. Using this refined mesh, the numerator and denominator of the Rayleigh quotient can be summed for each element. When all elements in the original finite element have been examined in this manner, the numerator can be divided by the denominator in the Rayleigh quotient to form a new eigenvalue.

The best use of this new eigenvalue is as an error measure for the original finite element analysis as the new eigenvalue is not guaranteed to be exact.

7. CONCLUSIONS

It has been demonstrated that the patch technique is suitable for obtaining an error estimation for the eigenvalue of a finite element natural frequency analysis. The method outlined in this paper has involved only beam and two-dimensional membrane elements. Structural models using finite elements for plate vibration [9], plate buckling [10], three-dimensional brick elements [11] and the vibration analysis using the finite strip method [12].

The least squares technique was used as the method of finding a higher order function than the finite element shape function for the vibrating shape over the elements. This method was used as it is computationally inexpensive. However, there is no guarantee on the shape producing a greatly improved result. Better interpolation procedures are required for this method with far more complex deformed shapes.

To obtain an error estimate for the natural frequency of a structure analyzed using the finite element method is relatively inexpensively achieved using the patch recovery technique shown in this paper. The calculation of the eigenvalue error is performed by

examining each element and a surrounding patch. This requires far less computational time than the eigenvalue extraction process for most finite element models. The patch recovery technique is not only effective but is also quite fast, and could be easily adopted by most finite element analysis codes as a post-processor routine to indicate the effectiveness of the finite element analysis.

ACKNOWLEDGMENTS

The first author is supported financially by the Australian Postgraduate Research Award (Industry) in conjunction with G + D Computing of Sydney.

REFERENCES

1. D. B. STEPHEN and G. P. STEVEN 1994 *Research Report, FEARC-9402, Finite Element Analysis Research Centre, University of Sydney*. Buckling error estimation using a patch recovery technique.
2. P. G. STRANG and G. J. FIX 1973 *An Analysis of the Finite Element Method*. Englewood Cliffs, NJ: Prentice-Hall.
3. J. DOUGLAS and T. DUPONT 1970 *SIAM Journal for Numerical Analysis* **4**, 575–626. Galerkin methods for parabolic problems.
4. E. HINTON and J. S. CAMPBELL 1974 *International Journal of Numerical Methods in Engineering* **8**, 461–480. Local and global smoothing of discontinuous finite element functions using a least square method.
5. O. C. ZIENKIEWICZ and J. Z. ZHU 1992 *International Journal of Numerical Methods in Engineering* **33**, 1331–1364. The superconvergent patch recovery and *a posteriori* error estimates, part 1: the recovery technique.
6. O. C. ZIENKIEWICZ and J. Z. ZHU 1992 *International Journal of Numerical Methods in Engineering* **33**, 1331–1364. The superconvergent patch recovery and *a posteriori* error estimates, part 2: error estimates and adaptivity.
7. N.-E. WIEBERG and X. D. LI 1994 *Communications in Numerical Methods in Engineering* **10**, 313–320. Superconvergent patch recovery of finite-element solution and *a posteriori* L_2 norm error estimate.
8. J. BARLOW 1976 *International Journal of Numerical Methods in Engineering* **10**, 243–251. Optimal stress location in finite element method.
9. D. B. STEPHEN and G. P. STEVEN 1997 *Engineering Computations*, to be published. Error estimation for natural frequency analysis using plate elements.
10. D. B. STEPHEN and G. P. STEVEN 1996 *Computers and Structures* **61**, 747–761. Error estimation for plate buckling elements.
11. D. B. STEPHEN and G. P. STEVEN 1997 *Structural Engineering and Mechanics*, to be published. Natural frequency error estimation for 3D brick elements.
12. D. B. STEPHEN and G. P. STEVEN 1997 *Journal of Sound and Vibration* **200**, 139–149. Error measures for the finite strip vibration analysis method.